Taylor & Francis
Taylor & Francis Group

Check for updates

BEDSIDE-TO-BENCH REPORT

Integration of radiotherapy with anti-PD-1 antibody for the treatment of intrahepatic or hilar cholangiocarcinoma: reflection from four cases

Qianqian Zhao[a]*, Yixing Chen[a]*, Shisuo Du[a], Xinrong Yang[b], Yanling Chen[c], Yuan Ji[d], and Zhaochong Zeng[a]

[a]Department of Radiation Oncology, Zhongshan Hospital, Fudan University, Shanghai, China; [b]Department of Liver Surgery and Liver Transplantation, Liver Cancer Institute, Zhongshan Hospital, Fudan University, Shanghai, China; [c]Department of Hepatobiliary Surgery, Fujian Medical University Union Hospital, Fuzhou, China; [d]Department of Pathology, Zhongshan Hospital, Fudan University, Shanghai, China

ABSTRACT

Cholangiocarcinoma (CCA) represents a clinically challenging disease with a dismal prognosis. A therapeutic plateau has been reached with traditional treatments. However, with immunotherapy advances in cancer therapy, integration of stereotactic body radiotherapy (SBRT) with anti-PD-1 antibody shows a synergistic effect and high clinical efficacy in many cancer types. This combination may represent a breakthrough in the treatment of this fatal malignancy. Here, we report four cases of refractory advanced intrahepatic or hilar cholangiocarcinoma that were successfully controlled with anti-PD-1 antibody following or concurrent with SBRT. Furthermore, one case was initially unresectable; however, following this novel combined therapy, it became operable. We discuss the challenges of developing predictive biomarkers for anti-PD-1 antibody responsiveness. We also consider the regulatory effect of SBRT on the tumor microenvironment and the potential advantages of this therapy combination for treatment of intrahepatic or hilar cholangiocarcinoma. These are important considerations and provide direction for future clinical trial designs.

Introduction

In recent years, with the improvement and development of imaging examinations, researchers found the increase of finding biliary tract cancers. Intrahepatic cholangiocarcinoma (ICC) is the second most common primary malignant tumor of the liver following only hepatocellular carcinoma (HCC) and it accounts for 10–20% of all primary liver cancer cases.[1] ICC has recently seen rapidly Growing interest due to its associated rising mortality and incidence worldwide.[2] Although complete operative resection is currently the primary potential radical treatment option, it is only achievable in less than one-third of patients at the time of presentation. Moreover, the prognosis remains dismal after curative resection, with a high recurrence rate of 40–80% and a 5-year survival rate of only 20–40%.[3–6] In addition, stereotactic body radiotherapy (SBRT) and radiofrequency ablation (RFA) were also used as the alternative treatment option for some small lesions. The combination of gemcitabine plus platinum-based compounds is the current first-line standard treatment for patients with advanced ICC, yet it has very limited therapeutic value with a median overall survival of less than 1 year.[7–10] There are other locoregional therapies such as, transarterial arterial chemoembolization (TACE), Y90, and RFA; however, current data support that these treatments were applied only in selected cases or as palliative therapy.[11,12] Furthermore, for the vast majority of patients with recurrent or metastatic disease, no standard effective treatment protocols are available.

Therefore, novel and effective therapeutic options are urgently required for this fatal malignancy.

With technological advances in radiation delivery, SBRT is a safe and effective therapeutic option for ICC patients with small lesions due to substantial local control and increased overall survival rates.[13] More encouragingly, immune checkpoint inhibitors (ICIs) targeting the PD-1 (programmed cell death protein 1)/PD-L1 (PD-1 ligand) pathway have recently provided a therapeutic revolution in cancer therapy and have shown excellent efficacy for a wide range of malignancies.[14–17] NCCN (National Comprehensive Cancer Network) guidelines recommend pembrolizumab as a choice for solid tumors with deficient mismatch repair (dMMR) or microsatellite instability (MSI-H), including biliary malignant tumor.[18] PD-1 blockades with RT or chemotherapy in ICC treatment had been investigated and exhibited promising therapeutic perspectives, although more evidence is still needed to confirm the efficacy.[19,20] The rationale behind the combined effect of radiotherapy with immunotherapy has also been investigated.[21–24]

Here, we report four cases of refractory advanced ICC or hilar cholangiocarcinoma that were successfully controlled with anti-PD-1 antibody following or concurrent with SBRT, which means that patients achieved complete response, partial response, or disease stable based on RECIST criteria. We also describe some remarkable findings during this combined strategy, including the hypereosinophilia and pseudoprogression. Furthermore, there was one case that was initially unresectable that became operable following this novel combined therapy.

Different from the previous reports, we further analyzed the changes of the expression tumor-infiltrating lymphocytes and PD-L1 on tumor tissue before and after radiotherapy to try to investigate the underlying mechanism of this combination therapy. Our report provides important considerations and direction for future clinical trial designs.

Case presentations

Case 1

A 50-year-old, previously healthy man visited Zhongshan Hospital, Fudan University due to liver masses detected during a routine physical examination in October 2017. The tumor biomarkers alpha-fetoprotein (AFP) (3.7 ng/mL) (normal range, < 20 ng/mL) and carcinoembryonic antigen (CEA) (3.1 ng/mL) (normal range, < 5 ng/mL) levels were within the normal limits; however, carbohydrate antigen 199 (CA199) was elevated with 50.5 U/mL (normal range, < 37 U/mL) (Figure 1). Magnetic resonance imaging (MRI) scans of the abdomen at presentation revealed two hepatic tumors with no significant

lymph nodes or distant metastases. One of the tumors was located in segment 2 (S2) of the liver with a maximum diameter of 3.4 cm and the other tumor was located in segment 5 (S5) with a maximum diameter of 0.9 cm (Figure 1a). The MRI showed a low-intensity mass on T1-weighted spin echo image and a high-intensity mass on T2-weighted. Enhanced MRI scans demonstrated a ring-like enhancement around the tumor in the early phase and a peripheral low-density area with a central low-density area in the late phase for the S2 lesion. Intense arterial enhancement followed by contrast washout was seen in the venous phase in the S5 lesion.

The physical examination was normal and the patient's Eastern Cooperative Oncology Group (ECOG) performance status was 0. The patient had a history of cirrhosis for 10 years and a personal history of excessive alcohol use for 30 years. On the basis of the above findings, ICC was suspected. The patient refused biopsy for diagnosis confirmation and surgical resection. RT was used as the alternative treatment with a total dose of 55 Gy and 60 Gy in 10 fractions to the S2 and S5 tumor lesions, respectively, between October 24 and November 3, 2017 (Figure 1b). Reevaluation by MRI 50 days after SBRT revealed that the
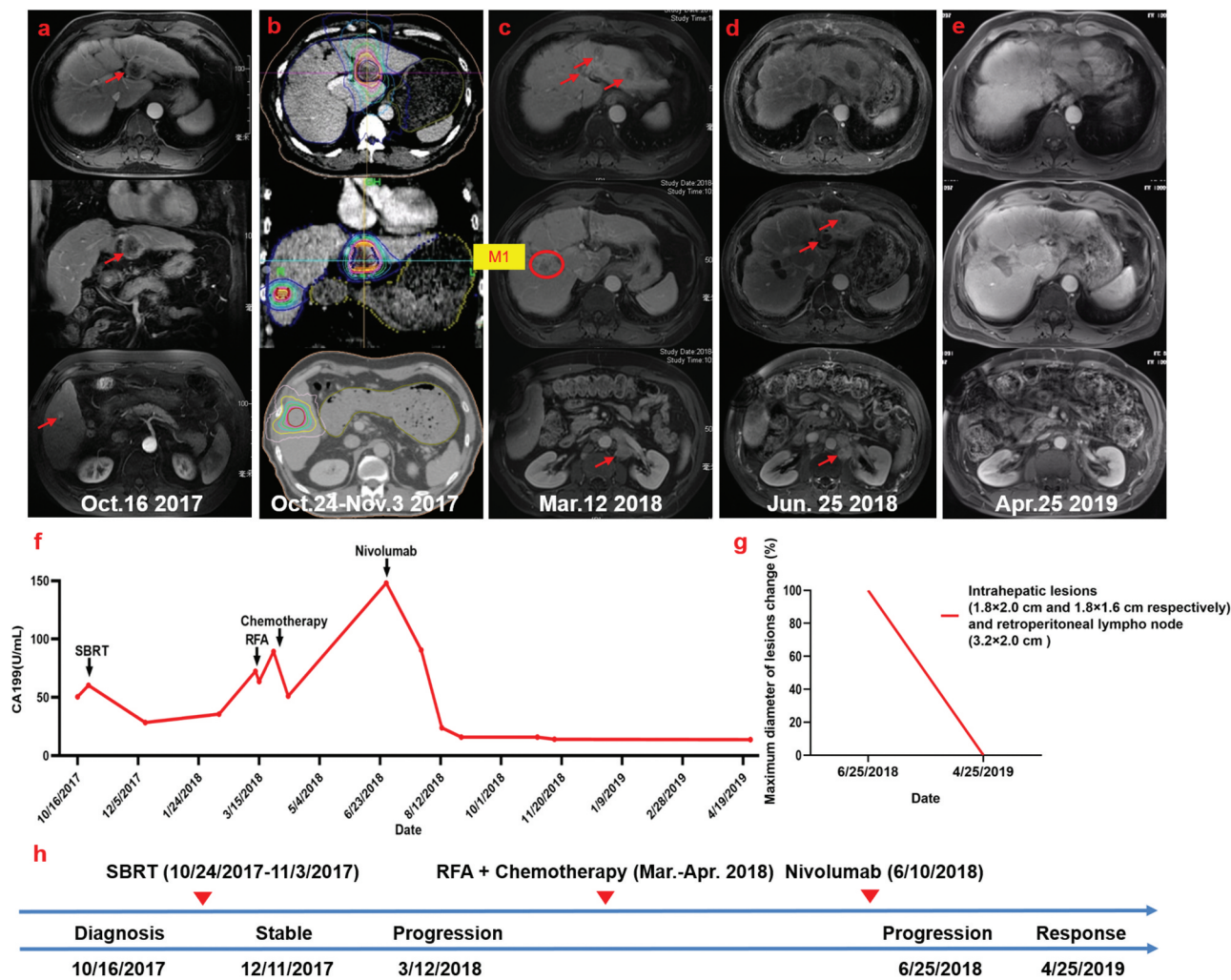

Figure 1. Summary of imaging scans and timeline of therapy and disease status for Case 1. (a) Patient status before treatment. (b) Radiotherapy (RT) planning. (c) Multiple new metastases and enlarged retroperitoneal lymph nodes emerged 4 months after SBRT. The patient then received radiofrequency ablation (RFA) and chemotherapy. (d) Further disease progression. (e) Remarkable regression of the lesions was seen following Nivolumab administration. (f) Serum carbohydrate antigen 199 (CA199) levels with respect to the treatment timeline. (g) Statistics of maximum diameter of lesions change for all lesions. Ten months after Nivolumab treatment, the patient achieved complete response (RECIST criteria). (h) Timeline showing therapy and disease status throughout the disease course.

lesions stabilized or shrank slightly. A dramatic decrease in the CA199 concentration was detected 2 months after SBRT (from 60.4 to 28.4 U/mL) (Figure 1f). Notably, at this time point, hypereosinophilia was evident based on a white blood cell count of 12.94×10^9 cells/L and an eosinophil count of 7.51×10^9 cells/L.

A second reevaluation by MRI in March 2018 showed multiple intrahepatic and extrahepatic metastases, including enlarged retroperitoneal lymph nodes, suggesting disease progression (Figure 1c). The patient underwent positron emission tomography-computed tomography (PET-CT) examination that showed: 1) a massive fluorodeoxyglucose (FDG) uptake and increased metabolic activity in multiple liver lesions with a maximum standard uptake value of 15.4, and 2) extensive involvement of the hepatic hilar, bilateral diaphragmatic feet, and retroperitoneal lymph nodes. The serum CA 199 level had increased to 63.7 U/mL at that time (Figure 1f).

Palliative radiofrequency ablation (RFA) for the de novo intrahepatic lesions was performed in March 2018 without complication. With the patient's consent, liver biopsy was performed (corresponding to the M1 lesion indicated by a red circle in the Figure 1c) during RFA treatment and the histopathology indicated ICC. Further immunohistochemical (IHC) staining of the tumor tissue showed high numbers of PD-L1 positive tumor cells (SP142 antibody) and abundant infiltration of $CD4^+$ and $CD8^+$ T cells (Figure S1). In addition, mismatch repair (MMR) testing showed proficient mismatch repair (pMMR), with a total mutation burden of 7.5 mut/Mb. Subsequently, the patient started systemic chemotherapy with a regimen of gemcitabine (1.5 g on days 1 and 8) and oxaliplatin (100 mg on days 1 and 8) every 3 weeks. However, after day 1 of the second cycle, chemotherapy was discontinued due to grade 3 myelosuppression.

The patient developed further disease progression shortly after chemotherapy discontinuation. An MRI scan in June 2018 indicated progressive enlargement of the masses in the liver, a new left adrenal gland metastasis, significant growth of enlarged retroperitoneal lymph nodes, and mild ascites (Figure 1d). Furthermore, the serum level of CA199 increased to 148 U/mL (Figure 1f). In light of the tumor PD-L1 expression level, PD-1 blockade with Nivolumab (3 mg/kg every 2 weeks) was initiated on June 10, 2018. In the follow-up imaging performed on August 29 and October 31, 2018, the intrahepatic lesions and retroperitoneal lymph nodes were stable and the left adrenal gland metastasis gradually shrank and finally disappeared. The elevated serum CA199 level prior to Nivolumab treatment (148 U/mL) dramatically declined to normal values after one month of treatment (24 U/mL) and remained within normal limits thereafter (<37 U/mL). At the time of the last follow-up in July 2019 (Figure 1f), the patient had continued to receive Nivolumab treatment for 10 months without any obvious autoimmune side effects. To date, there is no clinical evidence of disease progression.

Case 2

A 59-year-old man who had undergone left liver lobe resection for HCC (2.3 cm in diameter) in September 2005 presented at Zhongshan Hospital, Fudan University with a recurrent liver lesion detected in the patient's routine post-operative follow-up imaging in August 2018. AFP (1.5 ng/mL) and CEA (2.8 ng/

mL) levels were within the normal limits; however, the CA199 level was elevated to 71.3 U/mL (Figure 2h). Abdominal MRI scans on August 10, 2018 revealed an abnormal signal foci in the left liver lobe (Figure 2a). There was no significant lymph node or distant metastasis. The patient had a 10-year history of hypertension and diabetes; his ECOG performance status was 1.

After thorough discussion of treatment options, segment hepatectomy for resection of the recurrent lesion, complex enterolysis, and diaphragmatic repair were performed on August 15, 2018. Post-operative pathology revealed a 65×55 mm whitish tan mass with irregular margins. Microscopically, the tumor consisted of grade-III ICC; invasion of surgical margins was not observed (Figure S2). Peripheral hepatocyte steatosis was seen in 15% of the observed area. There was no residual lesion at the primary site and lymph nodes were not involved. IHC staining showed weak positive expression of PD-L1 (Figure S2). In addition, MMR testing results showed pMMR.

However, abdominal MRI scans on November 15, 2018 indicated that the disease had progressed with multiple new liver lesions (Figure 2b). At this time, the patient's CA199 level was 30.5 U/mL (Figure 2h). Subsequently, the patient started systemic chemotherapy with a regimen of paclitaxel (200 mg on days 1 and 8) and oxaliplatin (220 mg on day 1). The chemotherapy was well tolerated except for grade 1 diarrhea and alopecia. After two cycles of chemotherapy, MRI scans on January 3, 2019 revealed increased tumor size and number at all liver sites, a new increased right cardiodiaphragmatic angle, and renal hilus lymph nodes, demonstrating further disease progression (Figure 2c). In addition, a blood test showed the patient's CA199 level was elevated to 60.9 U/mL (Figure 2h).

The patient then received RT for the largest lesion (7.7 cm × 9.1 cm) on the left liver lobe with total doses of 50 Gy in 10 fractions from January 14 to January 26, 2019 (Figure 2d). Concurrently, Nivolumab (200 mg, every 2 weeks) was started on January 16, 2019. However, the patient's CA199 level continued to elevate during the treatment to 76.6 U/mL on February 18, 2019. Biopsy of the two unirradiated small liver lesions (corresponding to the M1 and M2 lesions indicated by red circles in Figure 2e) was performed on February 27, 2019. Histology showed ICC with pseudoprogression due to intense coagulation necrosis and diffusely infiltrating neutrophils (Figure S2). Further tests showed that 50% of the tumor cells staining positive using the SP142 antibody, which was higher than that of the tumor tissues obtained during the operation. The percentages of $CD4^+$ and $CD8^+$ infiltrating lymphocytes were also higher in metastatic lesions following SBRT than in the operative specimen.

In the follow-up MRI scans performed on March 28, 2019 (Figure 2f), the liver lesions were stabilized or slightly larger. However, two months later, MRI scans on June 10, 2019 showed marked shrinkage of the liver lesions (Figure 2g). Blood tests showed transient elevation of the serum CA199 levels to 240 U/mL 2 months after the initiation of Nivolumab treatment when the levels began to decrease (Figure 2h). To date, the patient is living with no disease progression and has continued Nivolumab treatment for 5 months, which has been tolerated well.
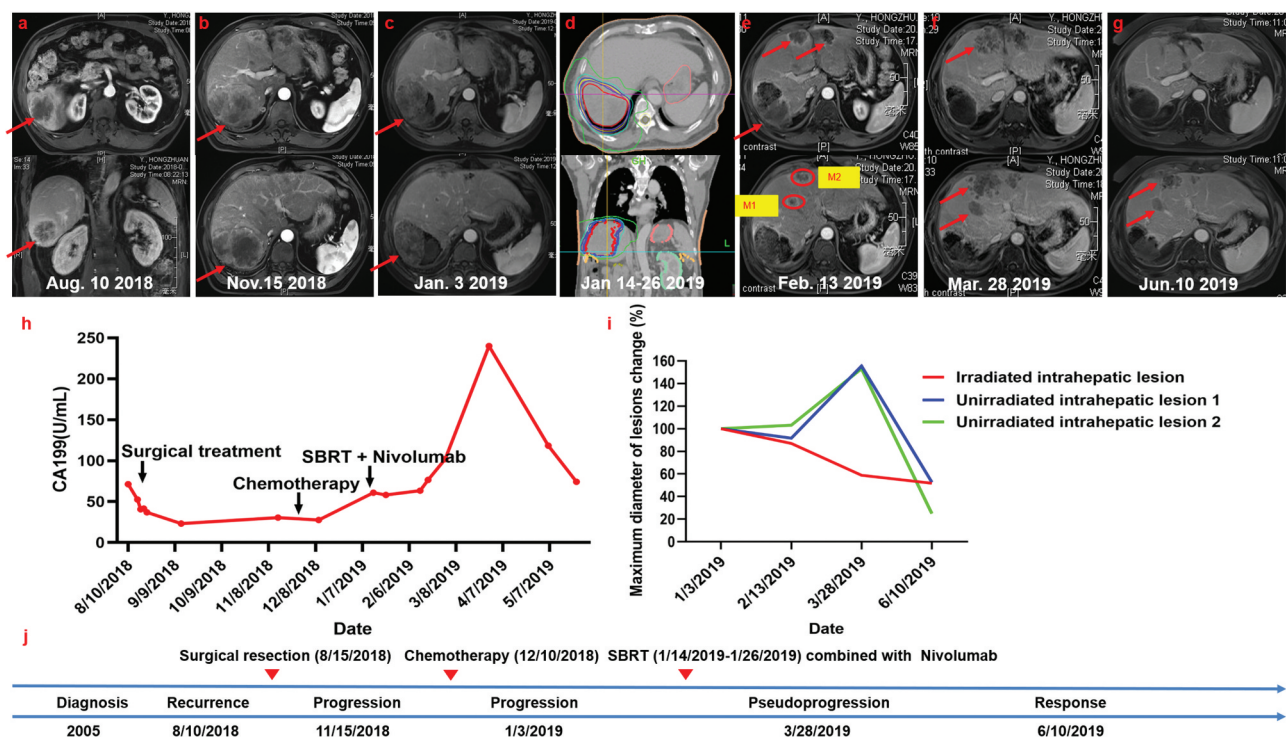
Figure 2. Summary of imaging scans and timeline of therapy and disease status for Case 2. (a) Baseline status before surgical resection. (b) MRI scans 2 months after operation revealed disease progression with multiple new liver lesions. The patient then received two cycles of chemotherapy. (c) MRI scans on January 3, 2019 revealed increases in size and numbers at all liver sites and new enlarged right cardiodiaphragmatic angle and renal hilus lymph nodes, thus demonstrating further disease progression. (d) Radiotherapy (RT) planning. (e and f) Transient increases in the size of lesions. (g) At the next assessment, the liver lesions had regressed, thus representing early pseudoprogression. (h) Serum carbohydrate antigen 199 (CA199) levels with respect to the treatment timeline. (i) Statistics of maximum diameter of lesions change for all lesions. Five months after Nivolumab treatment, the patient achieved partial response (RECIST criteria). (j) Timeline showing therapy and disease status throughout the disease course.

Case 3

A 65-year-old man underwent wide resection of hilar cholangio-carcinoma, as well as cholecystectomy and Roux-en-Y hepatico-jejunostomy at the Fujian Medical University Union Hospital in February 2015. Post-operative pathology revealed a moderately differentiated bile ductal adenocarcinoma in the hepatic portal measuring $30 \times 20 \times 20$ mm with invasion to adjacent adipose tissue, gallbladder wall, and nerve fibers. No hilar lymph node metastasis was found, but one of four lymph nodes showed metastasis in the fatty tissue surrounding the tumor. IHC staining showed almost no PD-L1 expression and low densities of CD4^{+} and CD8^{+} tumor-infiltrating lymphocytes (Figure S3).

The patient presented again at the Fujian Medical University Union Hospital in January 2018 after serum CA199 levels were elevated during a routine post-operative follow-up. Abdominal MRI scans on January 22, 2018 revealed an active focal lesion between the liver and stomach, which was suspected to be recurrent or metastatic (Figure 3a). There were no other significant lymph nodes or distant metastasis. CA199 and CEA levels were elevated to 192.20 U/mL and 8.5 ng/mL, respectively, on January 30, 2018 (Figure 3h). At the same time, a physical examination was normal and the patient's ECOG performance status was 0.

The patient then received palliative RT for the recurrent lesion with total doses of 35 Gy in 7 fractions between January 30, 2018

and February 7, 2018 (Figure 3b). However, PET-CT scans on June 20, 2019 indicated progressive enlargement of the recurrent lesion and growth of a new hepatic hilar metastasis (Figure 3c). At this time, blood tests showed that the CA199 level was 112.10 U/mL and the CEA level was elevated to 21.4 ng/mL (Figure 3h). Thus, the recurrent lesion was re-irradiation at a dose of 25 Gy in 5 fractions and the new hepatic hilar metastasis was concurrently irradiated at a dose of 50 Gy in 5 fractions from June 9 to June 15, 2018 (Figure 3d).

Despite these treatments, a left supraclavicular lymph node metastasis was detected by MRI on December 4, 2018 (Figure 3e). In addition, the patient's serum CA199 level was 60.9 U/mL and the CEA level was 37.1 ng/mL (Figure 3h). The patient then received RT for the left supraclavicular lymph node metastasis with total doses of 30 Gy in 3 fractions from December 11 to December 13, 2018 (Figure 3f). Concurrently Pembrolizumab treatment began on December 10, 2018 and was administered at 100 mg every 3 weeks. However, the CA199 level continued to elevate during the treatment and rose to 55.07 U/mL on March 20, 2019. At this time, CEA levels began to decrease to 36.6 ng/mL. Nivolumab was then introduced as an alternative therapy (140 mg, every 2 weeks) due to person reasons. After Nivolumab treatment of 4 months, images on April 17, 2019 showed that the serum levels of CA199 and CEA and the lesions became stable (Figure 3).
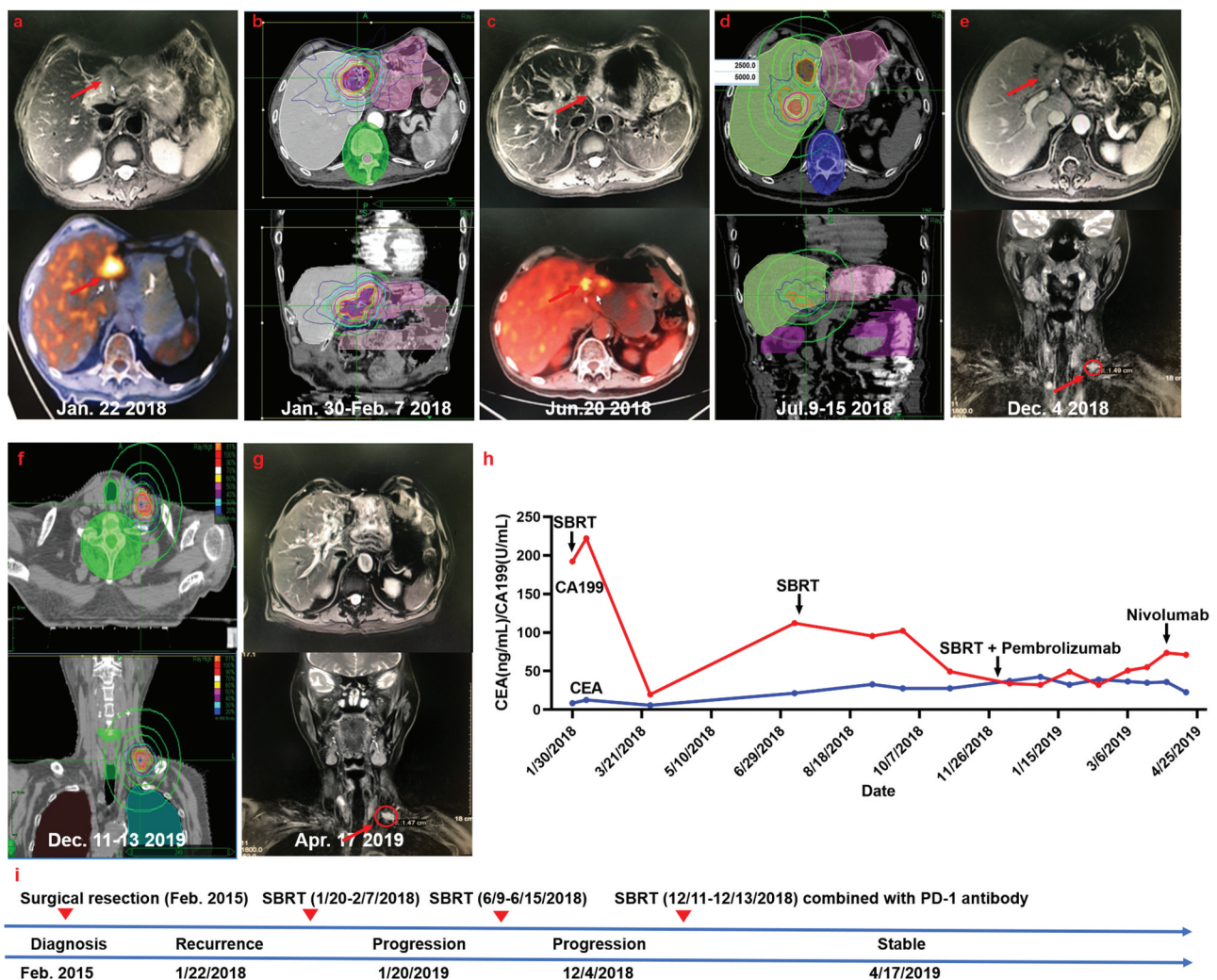
Figure 3. Summary of imaging scans and timeline of therapy and disease status for Case 3. (a) The recurrent status after surgical resection. (b) The patient then received stereotactic body radiotherapy (SBRT) for the recurrent lesion. (c) MRI scans 4 months after RT revealed progressive enlargement of the recurrent lesion and growth of a new hepatic hilar metastasis. (d) The second SBRT for the recurrent lesion and the new hepatic hilar metastasis. (e) Further disease progression with a left supraclavicular lymph node metastasis detectable in December 2019. (f) The third SBRT for the left supraclavicular lymph node metastasis. (g) The disease stabilized after anti-PD-1 immunotherapy administration. (h) Serum carbohydrate antigen 199 (CA199) and carcinoembryonic antigen (CEA) levels with respect to the treatment timeline. (i) Timeline showing therapy and disease status throughout the disease course.

Case 4

A 52-year-old, previously healthy, man initially presented to Zhongshan Hospital, Fudan University with the chief complaint of weight loss over 2 weeks in August 2018. The patient's CEA level was 3.1 ng/mL; however, AFP and CA199 levels were elevated to 833.6 ng/mL and 50.5 U/mL, respectively (Figure 4f). MRI scans of the abdomen on August 7, 2018 revealed a large lesion (12.9 × 11.8 cm) with multiple satellite lesions in the right hepatic lobe that extended to the right adrenal, upper pole of the right kidney, right posterior branches of the hepatic portal vein, right hepatic vein, and inferior vena cava, and hepatic hilar lymph node metastasis (Figure 4a). A subsequent PET scan on August 7, 2018 showed increased metabolic activity of the primary liver tumor and portal lymph nodes with no other significant lymph node or distant metastasis. The physical examination was normal and the patient's ECOG performance status was 0.

The patient then underwent liver biopsy, which confirmed ICC. Immunohistochemically, few cells were positive for PD-L1 (SP142 antibody), CD4, or CD8 (Figure S4). Considering the AFP level, the patient was diagnosed with combined ICC and HCC. Surgical treatment was not recommended due to the presence of satellite nodules and the tumor extension to neighboring tissues.

The primary tumor was treated with RT at a total dose of 36 Gy in 12 fractions between August 15 and August 31, 2018. Radiographic imaging on September 19, 2018 revealed a decrease in the size of the target lesions (Figure 4b). On October 9, 2018, treatment with Pembrolizumab (2 mg/kg every 3 weeks) combined with Everolimus (5 mg every day) was initiated. After one week of treatment, AFP levels returned to normal and CA199 levels declined to 82.2 U/mL (Figure 4f). The follow-up MRI scans performed after 3 months of treatment on December 27, 2018, showed
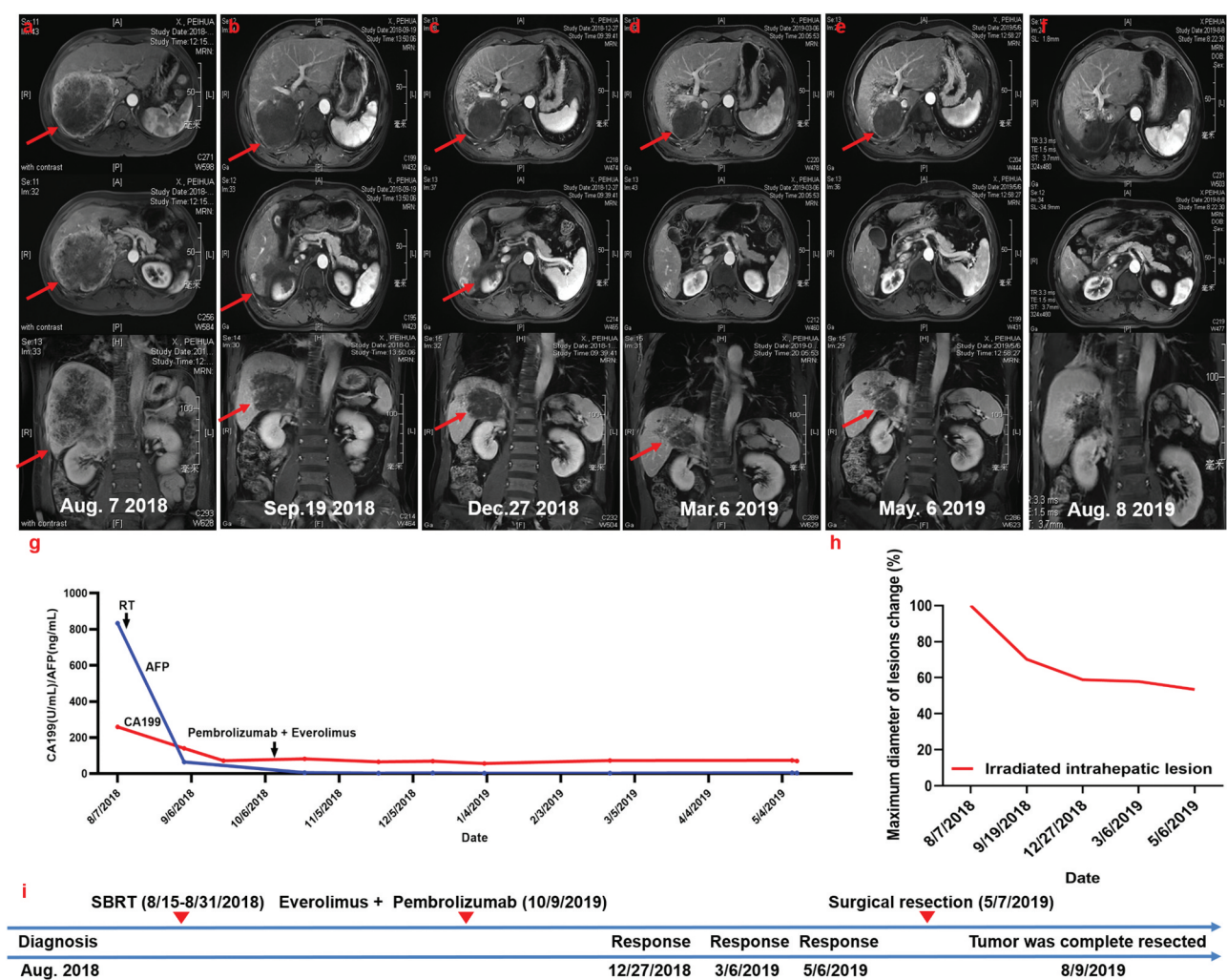
Figure 4. Summary of imaging scans and timeline of therapy and disease status for Case 4. (a) Baseline status before treatment with Nivolumab and radiotherapy (RT). (b) MRI images 20 days after radiotherapy revealed decreased size of the radiation-targeted lesion. (c, d, and e) Evidence of complete remission after treatment with Everolimus combined with Pembrolizumab. The patient then underwent radical surgical resection. (f) MRI scans obtained 3 months after surgical resection showed that the tumor was complete resected. (g) Serum carbohydrate antigen 199 (CA199) and alpha-fetoprotein (AFP) levels with respect to the treatment timeline. (h) Statistics of maximum diameter of the lesion. Seven months after Nivolumab treatment, the patient achieved partial response (RECIST criteria). (i) Timeline showing therapy and disease status throughout the disease course.

evidence of complete remission with the tumor burden considerably decreased (Figure 4c). Serum AFP levels declined from 65.3 ng/mL to 5.9 ng/mL and remained within normal limits (<20 ng/mL) thereafter. The CA199 level declined from 82.2 U/mL to 57.1 U/mL (Figure 4f). The subsequent imaging scans obtained in March and May 2019 showed further evidence of clinical responses (Figure 3d,e).

Based on the size reduction, a surgical resection was performed that included cholecystectomy and a partial diaphragm resection on May 7, 2019. Microscopic pathological examination showed that R0 resection (no residual tumor) had been successful and that more than 50% of the tumor cells were undergoing extensive tumor necrosis. Further tests showed that PD-L1 expression was extremely low, similar to the baseline biopsy. However, the percentages of CD4$^+$ and CD8$^+$ infiltrating lymphocytes were higher in the operative specimen than in the baseline biopsy specimen. The patient has made a remarkable recovery.

Discussion

ICC represents a difficult disease to treat, resulting in a very poor prognosis. Almost all ICC cases exhibit disease progression within a few months after commencing traditional treatments,[25] as was the case with the first three patients we presented here. Therefore, exploration of novel, effective treatment strategies is imperative. The ICC cases described here indicate that a combination strategy of SBRT with anti-PD-1 antibody had favorable anti-tumor activity and sustained clinical efficacy with a favorable safety profile. The median overall survival of these patients was greater than 1 year, much longer than that of advanced ICC patients treated with other traditional treatments.[3,5] In addition, Case 1 showed hypereosinophilia following SBRT, which may be associated with a favorable response to Nivolumab. Case 2 indicated a unique response pattern of pseudoprogression during the course of treatment with Nivolumab. Moreover, Case 4 indicated that radical surgical resection could be performed following this

novel combined strategy for initially unresectable, advanced ICC.

Anti-PD-1 antibody has recently become increasingly popular for cancer treatment. However, with most tumor entities, only approximately 20% of all patients show a sufficient treatment response.[26] In addition, considering the high treatment expenses and potential toxicities associated with these inhibitors, it is essential to select and identify good candidates for anti-PD-1 antibody. PD-L1 expression has been widely studied as a potential biomarker in clinical trials; however, PD-L1 expression is discordant, unstable, and dynamic due to tumor heterogeneity and sampling variability.[26] A lack of validated detection methods and a reliable definition of high PD-L1 expression levels make anti-PD-1 antibody more complex in the clinical setting.[27,28] Interestingly, studies have reported that some patients who are PD-L1 negative still obtain clinical efficacy with anti-PD-(L)1 therapies.[29,30] Thus, the predictive value of PD-L1 expression alone is currently debated and remains a challenge. Beyond PD-L1 expression, tumor mutation burden, mismatch repair-deficient/microsatellite instability-high, and dense infiltration of cytotoxic T cells have also been suggested to be predictive biomarkers of successful anti-PD-1 antibody.[26,31–33] Furthermore, different studies have reported controversial predictive roles of these biomarkers in different tumor types. For MMR, only Cases 1 and 2 were proficient, but all four cases showed good clinical efficacy to Nivolumab. Cases 1 and 2 had relatively high PD-L1 expression levels and redundant lymphocyte and inflammatory cell infiltration following SBRT, which may be associated with their excellent responses and clinical efficacy. However, Cases 3 and 4 had very few PD-L1 positive cells in the tumor tissues. Taken together with the results of previous reports and our cases,[26,32] we hypothesize that anti-PD-1 antibody relies on multiple complex interactions and that the combined biomarkers may be more reliable in predicting a sustained response to immunotherapy in ICC patients.

A secondary analysis of the KEYNOTE-001 trial showed that patients who received any RT prior to Pembrolizumab had longer survival than those who did not.[34] This finding suggests that RT may generate a tumor-specific memory immune response, thus enhancing the anti-tumor response of ICIs after RT. Some studies have explored the underlying mechanisms of these responses. First, radiation can enhance tumor antigen expression and antigen presentation.[35] Radiation-induced immunogenic cell death can function as an "in situ" vaccine at the tumor site that improves the ability of effector T cells to recognize and kill tumor cells. Second, radiation can reprogram the tumor microenvironment (TME) to be favorable to effector T-cell recruitment and function.[35] Increased infiltration of lymphocytes effectively converts tumors into "inflamed" tissues that are susceptible to T-cell activation and attack. Unfortunately, due to a lack of tissue samples collected before or after SBRT in Cases 1 and 3, respectively, we could not investigate the effect of RT on the TME in these two patients. However, the dynamic TME following RT in Cases 2 and 4 validated the shaping capability of RT on the TME in ICC patients. Third, decreased tumor burden is associated with highly effective responses to immunotherapy.[36] The decreased tumor burden induced by RT in our reported cases may contribute to enhanced responses to the followed PD-1 antibody immunotherapy.

Several reports have indicated the inhibition of anti-tumor immunity induced by RT resulting in up-regulation of PD-L1 expression, up-regulation of vascular endothelial growth factor (VEGF), and direct toxicity to circulating lymphocytes.[37–39] These effects could curb anti-tumor immune responses and contribute to tumor progression. PD-L1 expression within the tumor front is associated with a 60% decrease in survival of ICC patients.[40] However, the negative effect of RT on anti-tumor immunity may be counterbalanced by the effect of anti-PD-1 antibody. For instance, the upregulated PD-L1 expression induced by RT may be overcome by the application of PD-(L)1 blockers, resulting in synergistic anti-tumor activity to eliminate the tumors. Thus, understanding the interactions between RT and anti-PD-1 antibody in ICC patients is of the utmost importance for maximizing therapeutic benefits.

Eosinophils play a pivotal role in tumor surveillance and are described as effectors for tumor rejection in animal models.[41–43] A high relative peripheral blood eosinophil count prior to treatment or an increase during treatment is associated with favorable overall survival in melanoma patients treated with Ipilimumab or Pembrolizumab, respectively.[44,45] This association has also been observed among cancer patients treated with IL-2, IL-4, and GM-CSF.[46–48] In Case 1, laboratory data showed transient elevation of the serum eosinophil count to 7.5×10^9 cells/L 50 days after the completion of SBRT with the baseline counts of 0.69×10^9 cells/L. It is difficult to determine whether this eosinophilia was secondary due to RT-induced immunogenicity effects. However, we hypothesize that the elevated level of eosinophils may have been involved in tumor eradication and may be associated with the positive responses to immunotherapy.

Several limitations should be noted in interpreting our study. First, because the cases and the data were limited, the results may not be representative of a broader population of ICC patients. Second, due to the invasiveness of sampling, the tumor tissue before and after RT was not always attainable. It is unknown whether PD-L1 expression changed following SBRT in Cases 1 and 3. Third, the fourth case was diagnosed as combined ICC and HCC, not ICC. At last, data on this combination strategy for cholangiocarcinoma patients are scarce. At present, there is one clinical trial exploring the efficacy and safety of this combined strategy for unresectable ICC (https://clinicaltrials.gov/, NCT03898895) worldwide. Though these four cases provide a starting point, additional clinical trials evaluating this treatment strategy are needed to better elucidate the treatment effect. Further evidence and prospective studies should be conducted to verify our findings.

Conclusion

Our cases showed that integration of SBRT with anti-PD-1 antibody may have a great effect on ICC. Furthermore, this combination therapy was well tolerated with no severe adverse events observed during therapy. This regimen may provide a new therapeutic option and represents a promising potential

treatment for ICC. Additionally, this combination therapy may make initially inoperable cases candidates for successful resection.

Disclosure of Potential Conflicts of Interest

No potential conflicts of interest were disclosed.

References

1. Razumilava N, Gores GJ. Cholangiocarcinoma. Lancet. 2014;383:2168–2179.
2. Bridgewater J, Galle PR, Khan SA, Llovet JM, Park JW, Patel T, Timothy M Pawlik, Gregory J Gores. Guidelines for the diagnosis and management of intrahepatic cholangiocarcinoma. J Hepatol. 2014;60:1268–1289.
3. Spolverato G, Kim Y, Alexandrescu S, Marques HP, Lamelas J, Aldrighetti L, Clark Gamblin T, Maithel SK, Pulitano C, Bauer TW, et al. Management and outcomes of patients with recurrent intrahepatic cholangiocarcinoma following previous curative-intent surgical resection. Ann Surg Oncol. 2016;23:235–243.
4. Hyder O, Hatzaras I, Sotiropoulos GC, Paul A, Alexandrescu S, Marques H, Pulitano C, Barroso E, Clary BM, Aldrighetti L, et al. Recurrence after operative management of intrahepatic cholangiocarcinoma. Surgery. 2013;153:811–818.
5. Wang Y, Li J, Xia Y, Gong R, Wang K, Yan Z, Wan X, Liu G, Wu D, Shi L, et al. Prognostic nomogram for intrahepatic cholangiocarcinoma after partial hepatectomy. J Clin Oncol. 2013;31:1188–1195.
6. Wirth TC, Vogel A. Surveillance in cholangiocellular carcinoma. Best Pract Res Clin Gastroenterol. 2016;30:987–999.
7. Valle J, Wasan H, Palmer DH, Cunningham D, Anthoney A, Maraveyas A, Madhusudan S, Iveson T, Hughes S, Pereira SP, et al. Cisplatin plus gemcitabine versus gemcitabine for biliary tract cancer. N Engl J Med. 2010;362:1273–1281.
8. Sahu S, Sun W. Targeted therapy in biliary tract cancers-current limitations and potentials in the future. J Gastrointest Oncol. 2017;8:324–336.
9. Bupathi M, Ahn DH, Bekaii-Saab T. Therapeutic options for intrahepatic cholangiocarcinoma. Hepatobiliary Surg Nutr. 2017;6:91–100.
10. Galle PR. Treating hepatobiliary cancers: the oncology way. Dig Dis. 2017;35:384–386.
11. Shindoh J. Ablative therapies for intrahepatic cholangiocarcinoma. Hepatobiliary Surg Nutr. 2017;6:2–6.
12. Sommer CM, Kauczor HU, Pereira PL. Locoregional therapies of cholangiocarcinoma. Visc Med. 2016;32:414–420.
13. Brunner TB, Blanck O, Lewitzki V, Abbasi-Senger N, Momm F, Riesterer O, Duma MN, Wachter S, Baus W, Gerum S, et al. Stereotactic body radiotherapy dose and its impact on local control and overall survival of patients for locally advanced intrahepatic and extrahepatic cholangiocarcinoma. Radiother Oncol. 2019;132:42–47.
14. Chiramel J, Tay R, Califano R. Durvalumab after chemo-radiotherapy in stage III non-small cell lung cancer. J Thorac Dis. 2018;10:S991–s4.
15. Janjigian YY, Bendell J, Calvo E, Kim JW, Ascierto PA, Sharma P, Ott PA, Peltola K, Jaeger D, Evans J, et al. CheckMate-032 study: efficacy and safety of nivolumab and nivolumab plus ipilimumab in patients with metastatic esophagogastric cancer. J Clin Oncol. 2018;36:2836–2844.
16. Koshkin VS, Barata PC, Zhang T, George DJ, Atkins MB, Kelly WJ, Vogelzang NJ, Pal SK, Hsu J, Appleman LJ, et al. Clinical activity of nivolumab in patients with non-clear cell renal cell carcinoma. J Immunother Cancer. 2018;6:9.
17. Kang YK, Boku N, Satoh T, Ryu MH, Chao Y, Kato K, Chung HC, Chen JS, Muro K, Kang WK, et al. Nivolumab in patients with advanced gastric or gastro-oesophageal junction cancer refractory to, or intolerant of, at least two previous chemotherapy regimens (ONO-4538-12, ATTRACTION-2): a randomised, double-blind, placebo-controlled, phase 3 trial. Lancet. 2017;390:2461–2471.
18. Le DT, Durham JN. Mismatch repair deficiency predicts response of solid tumors to PD-1 blockade. Science. 2017;357:409–413.
19. Sui M, Li Y, Wang H, Luo Y, Wan T, Wang X, Hu B, Cheng Y, Lv X, Xin X, et al. Two cases of intrahepatic cholangiocellular carcinoma with high insertion-deletion ratios that achieved a complete response following chemotherapy combined with PD-1 blockade. J Immunother Cancer. 2019;7:125.
20. Liu X, Yao J, Song L, Zhang S, Huang T, Li Y. Local and abscopal responses in advanced intrahepatic cholangiocarcinoma with low TMB, MSS, pMMR and negative PD-L1 expression following combined therapy of SBRT with PD-1 blockade. J Immunother Cancer. 2019;7:204.
21. Wang Y, Liu ZG, Yuan H, Deng W, Li J, Huang Y, Kim BYS, Story MD, Jiang W. The reciprocity between radiotherapy and cancer immunotherapy. Clin Cancer Res. 2019;25:1709–1717.
22. Stamell EF, Wolchok JD, Gnjatic S, Lee NY, Brownell I. The abscopal effect associated with a systemic anti-melanoma immune response. Int J Radiat Oncol Biol Phys. 2013;85:293–295.
23. Golden EB, Demaria S, Schiff PB, Chachoua A, Formenti SC. An abscopal response to radiation and ipilimumab in a patient with metastatic non-small cell lung cancer. Cancer Immunol Res. 2013;1:365–372.
24. Ko EC, Raben D, Formenti SC. The Integration of Radiotherapy with Immunotherapy for the Treatment of Non-Small Cell Lung Cancer. Clin Cancer Res. 2018;24:5792–5806.
25. Morise Z, Sugioka A, Tokoro T, Tanahashi Y, Okabe Y, Kagawa T, Takeura C. Surgery and chemotherapy for intrahepatic cholangiocarcinoma. World J Hepatol. 2010;2:58–64.
26. Teng F, Meng X, Kong L, Yu J. Progress and challenges of predictive biomarkers of anti PD-1/PD-L1 immunotherapy: A systematic review. Cancer Lett. 2018;414:166–173.
27. Hansen AR, Siu LL. PD-L1 testing in cancer: challenges in companion diagnostic development. JAMA Oncol. 2016;2:15–16.
28. Sacher AG, Gandhi L. Biomarkers for the Clinical Use of PD-1/PD-L1 Inhibitors in Non-Small-Cell Lung Cancer: A Review. JAMA Oncol. 2016;2:1217–1222.
29. Brahmer J, Reckamp KL, Baas P, Crino L, Eberhardt WE, Poddubskaya E, Antonia S, Pluzanski A, Vokes EE, Holgado E, et al. Nivolumab versus docetaxel in advanced squamous-cell non-small-cell lung cancer. N Engl J Med. 2015;373:123–135.
30. Robert C, Long GV, Brady B, Dutriaux C, Maio M, Mortier L, Hassel JC, Rutkowski P, McNeil C, Kalinka-Warzocha E, et al. Nivolumab in previously untreated melanoma without BRAF mutation. N Engl J Med. 2015;372:320–330.
31. Diaz LA Jr., Le DT PD-1. Blockade in tumors with mismatch-repair deficiency. Blockade Tumors Mismatch-Repair Deficiency. 2015;373:1979.
32. Maleki Vareki S, Garrigos C, Duran I. Biomarkers of response to PD-1/PD-L1 inhibition. Crit Rev Oncol Hematol. 2017;116:116–124.
33. Chalmers ZR, Connelly CF, Fabrizio D, Gay L, Ali SM, Ennis R, Schrock A, Campbell B, Shlien A, Chmielecki J, et al. Analysis of 100,000 human cancer genomes reveals the landscape of tumor mutational burden. Genome Med. 2017;9:34.
34. Shaverdian N, Lisberg AE, Bornazyan K, Veruttipong D, Goldman JW, Formenti SC, Garon EB, Lee P. Previous radiotherapy and the clinical activity and toxicity of pembrolizumab in the treatment of non-small-cell lung cancer: a secondary analysis of the KEYNOTE-001 phase 1 trial. Lancet Oncol. 2017;18:895–903.
35. Herrera FG, Bourhis J, Coukos G. Radiotherapy combination opportunities leveraging immunity for the next oncology practice. CA Cancer J Clin. 2017;67:65–85.
36. Huang AC, Postow MA, Orlowski RJ, Mick R, Bengsch B, Manne S, Xu W, Harmon S, Giles JR, Wenz B, et al. T-cell invigoration to tumour burden ratio associated with anti-PD-1 response. Nature. 2017;545:60–65.
37. Li T, Zeng ZC, Wang L, Qiu SJ, Zhou JW, Zhi XT, Yu HH, Tang ZY. Radiation enhances long-term metastasis potential of residual hepatocellular carcinoma in nude mice through TMPRSS4-induced

epithelial-mesenchymal transition. Cancer Gene Ther. 2011;18:617–626.

38. Zhao Q, Xu X, Yue J, Zhu K, Feng R, Jiang S, Qi Z, Wang R. Minimum absolute lymphocyte counts during radiation are associated with a worse prognosis in patients with unresectable hepatocellular carcinoma. Therap Adv Gastroenterol. 2017;10:231–241.

39. Deng L, Liang H, Burnette B, Beckett M, Darga T, Weichselbaum RR, Fu YX. Irradiation and anti-PD-L1 treatment synergistically promote antitumor immunity in mice. J Clin Invest. 2014;124:687–695.

40. Gani F, Nagarajan N, Kim Y, Zhu Q, Luan L, Bhaijjee F, Anders RA, Pawlik TM. Program death 1 immune checkpoint and tumor microenvironment: implications for patients with intrahepatic cholangiocarcinoma. Ann Surg Oncol. 2016;23:2610–2617.

41. Simson L, Ellyard JI, Dent LA, Matthaei KI, Rothenberg ME, Foster PS, Smyth MJ, Parish CR. Regulation of carcinogenesis by IL-5 and CCL11: a potential role for eosinophils in tumor immune surveillance. J Immunol. 2007;178:4222–4229.

42. Ikutani M, Yanagibashi T, Ogasawara M, Tsuneyama K, Yamamoto S, Hattori Y, Kouro T, Itakura A, Nagai Y, Takaki S, et al. Identification of innate IL-5-producing cells and their role in lung eosinophil regulation and antitumor immunity. J Immunol. 2012;188:703–713.

43. Carretero R, Sektioglu IM, Garbi N, Salgado OC, Beckhove P, Hammerling GJ. Eosinophils orchestrate cancer rejection by normalizing tumor vessels and enhancing infiltration of CD8(+) T cells. Nat Immunol. 2015;16:609–617.

44. Weide B, Martens A, Hassel JC, Berking C, Postow MA, Bisschop K, Simeone E, Mangana J, Schilling B, Di Giacomo AM, et al. Baseline biomarkers for outcome of melanoma patients treated with pembrolizumab. Clin Cancer Res. 2016;22:5487–5496.

45. Martens A, Wistuba-Hamprecht K, Geukes Foppen M, Yuan J, Postow MA, Wong P, Romano E, Khammari A, Dreno B, Capone M, et al. Baseline peripheral blood biomarkers associated with clinical outcome of advanced melanoma patients treated with ipilimumab. Clin Cancer Res. 2016;22:2908–2918.

46. Lotfi R, Lee JJ, Lotze MT. Eosinophilic granulocytes and damage-associated molecular pattern molecules (DAMPs): role in the inflammatory response within tumors. J Immunother. 2007;30:16–28.

47. Davis BP, Rothenberg ME. Eosinophils and cancer. Cancer Immunol Res. 2014;2:1–8.

48. Gatault S, Legrand F, Delbeke M, Loiseau S, Capron M. Involvement of eosinophils in the anti-tumor response. Cancer Immunol Immunother. 2012;61:1527–1534.